The impact of spatiotemporal detailing the forest LAI

CAMAERA GA meeting June 2025

Dr. H J. Jonas, Dr. L. Geers, Dr. X. Ge,
R. Kranenburg, Dr. M. Schaap

Leaf Area Index & dry-deposition

Leaf Area Index = the area of leaves per area (earth) [m^2/m^2]

- dry-deposition scheme in DEPAC/LOTOS-EUROS:
  - Aerodynamic Resistance — Ra
  - Quasi-Laminar Layer Resistance — Rb
  - Canopy Resistance — $Rc = (1/Rw + 1/Rs + 1/Rsoil)^{-1}$
    1. external leaf surface — Rw (LAI)
    2. stomata — Rs (LAI)
    3. soil — Rsoil_eff (LAI)
- Higher LAI > more dry-deposition

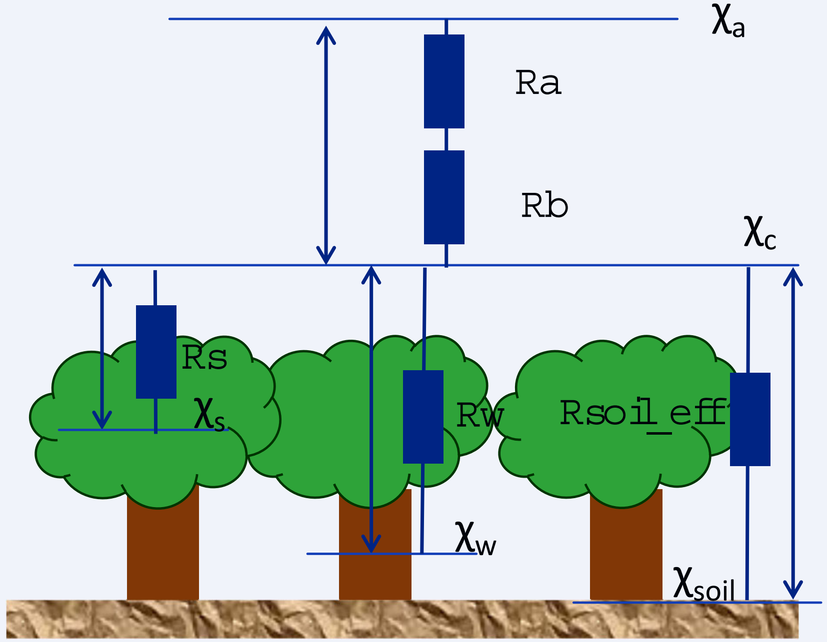

(van Zanten et al., 2010)

goals of this study:

- inspect spatiotemporal variability of forest LAI
- test sensitivity of this improvement

outline

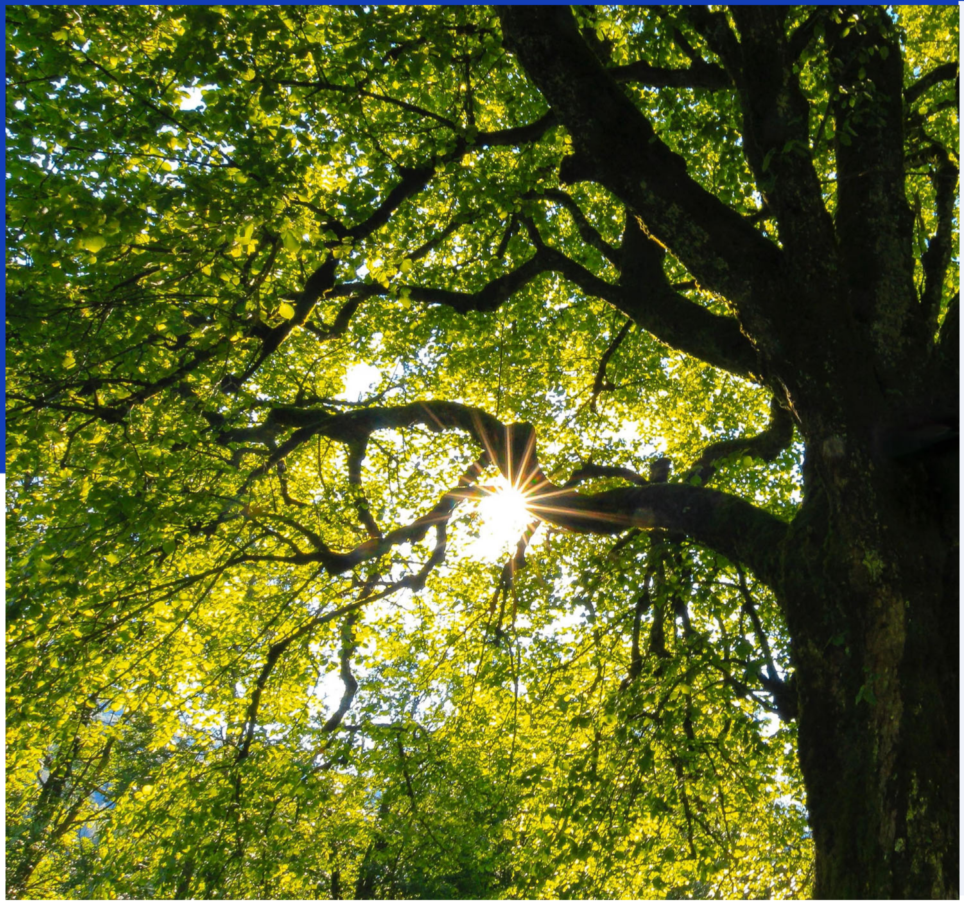

1. Spatiotemporal variability in satellite-derived LAI
   a. Masking and rescaling the satellite-dataset
   b. Spatial and temporal effects
2. Sensitivity Run in LOTOS-EUROS
   a. deposition scheme in LOTOS-EUROS
   b. simulation details
   c. impact of forest LAI on
      - *NHx and NOy dry-deposition*
      - *nitrate and ammonium aerosol formation*
   d. conclusions
3. Outlook

Masking the satellite data

- only those cells with >90% tree coverage are selected to represent the area
- the domain is divided in blocks
- LAI is averaged in each block

red = coniferous trees
blue = broadleaf trees

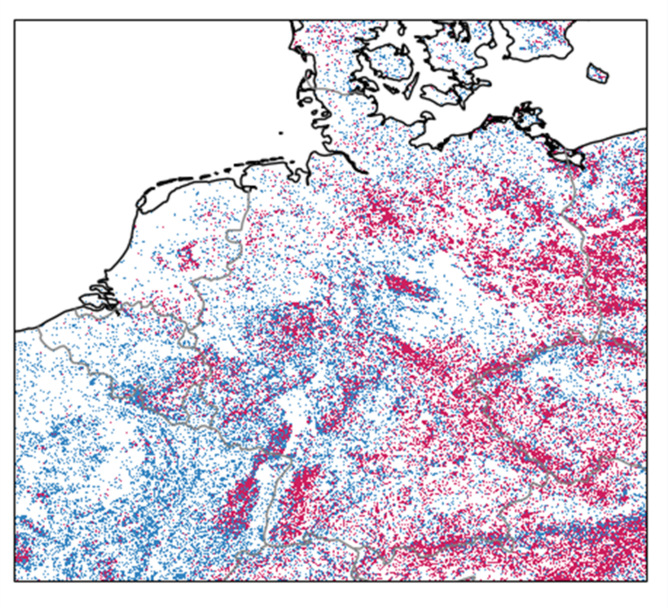

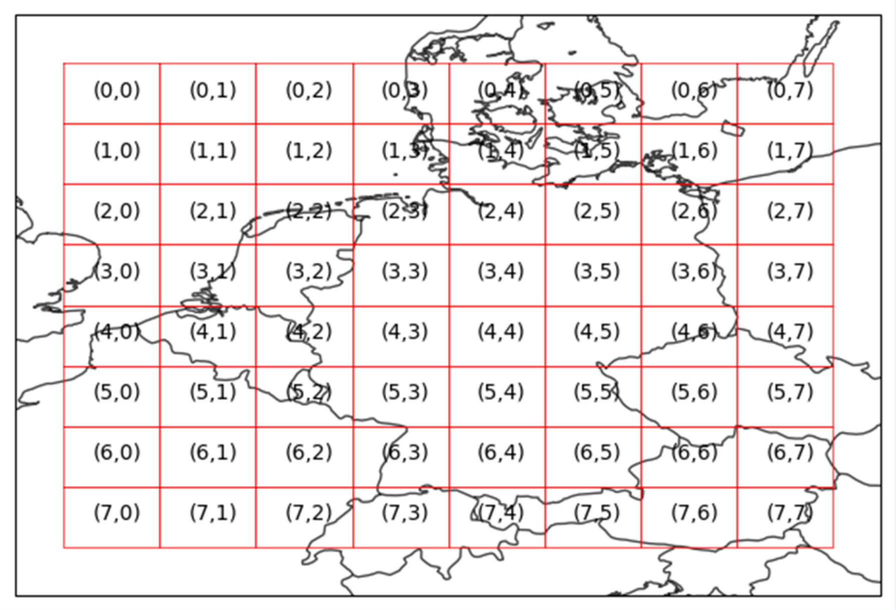

tree type map
- Copernicus 10x10m resolution from 2018
- coniferous and broadleaf trees
- DOI: https://doi.org/10.2909/7b28d3c1-b363-4579-9141-bdd09d073fd8

GEOV2: reprocessed MODIS leaf area index dataset
- 1x1 km resolution
- 1999-01 – 2020-06
- Int.J.Appl.Earth Obs.Geoinf.123 (2023) 103479

Rescaling the data

The satellite-derived LAI shows anomalies based on the properties of broadleaf and coniferous trees

- broadleaf: LAI ≠ 0 in winter
- coniferous: LAI ≠ constant

Therefore, we opt for a rescaling to retain spatiotemporal variability and tree properties.

$$\mathrm{LAI}(t,\mathrm{lon},\mathrm{lat}) = \begin{cases} (\mathrm{LAI} - \min_t \mathrm{LAI})\,\frac{\max_t \mathrm{LAI}}{\max_t \mathrm{LAI} - \min_t \mathrm{LAI}}, & \text{deciduous trees} \\ \max_t \mathrm{LAI}, & \text{evergreen trees} \end{cases}$$

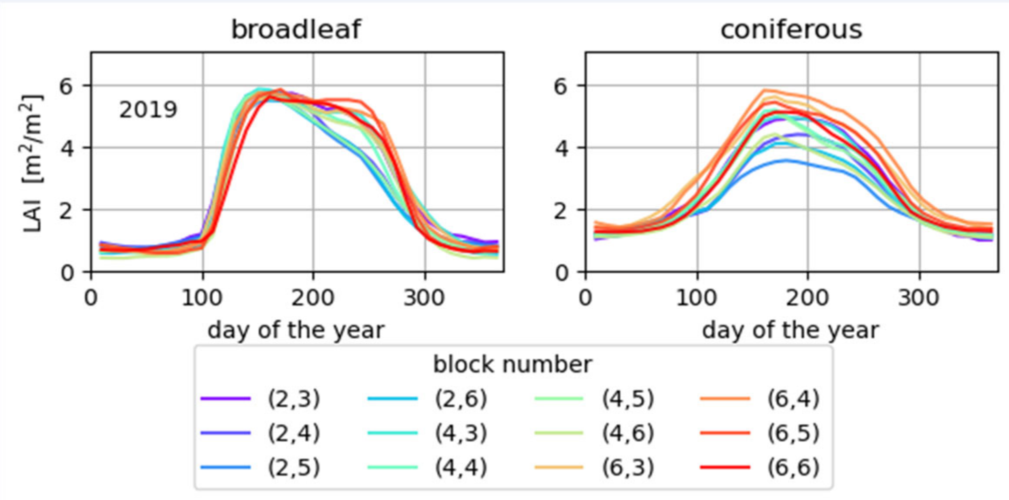

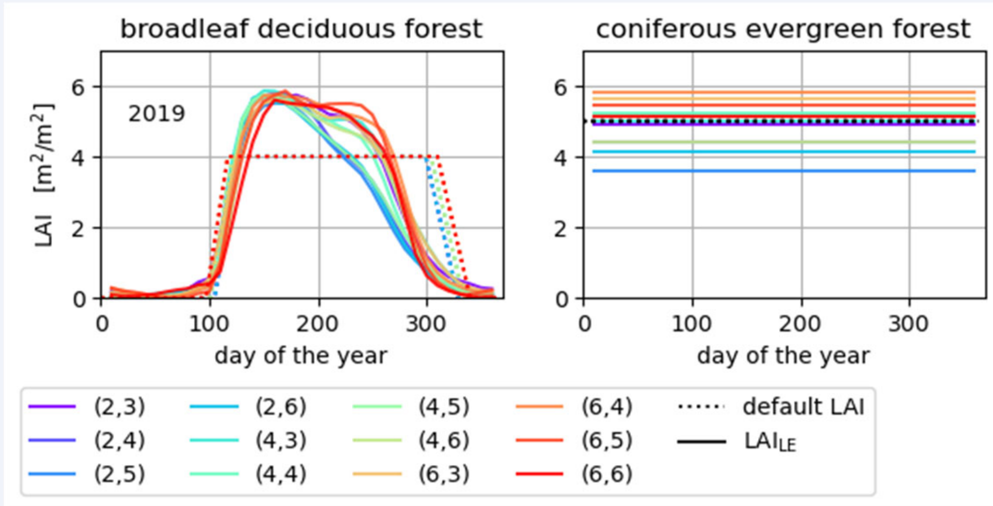

Temporal and spatial variability

- 2003: warm and dry summer -> faster decay
- 2011: warm spring and winter and excessive rainfall -> early LAI growth
- spatial variability seen in plateaus/decay in summer

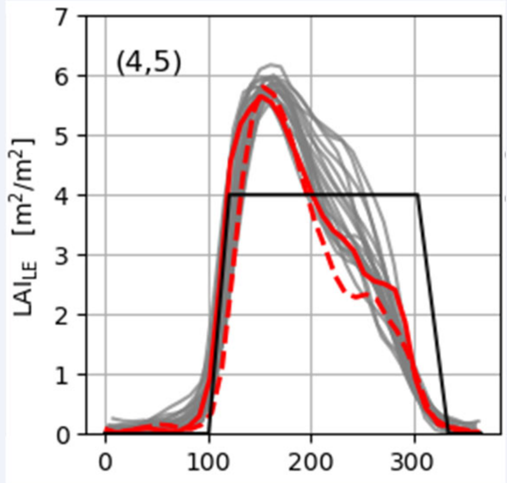

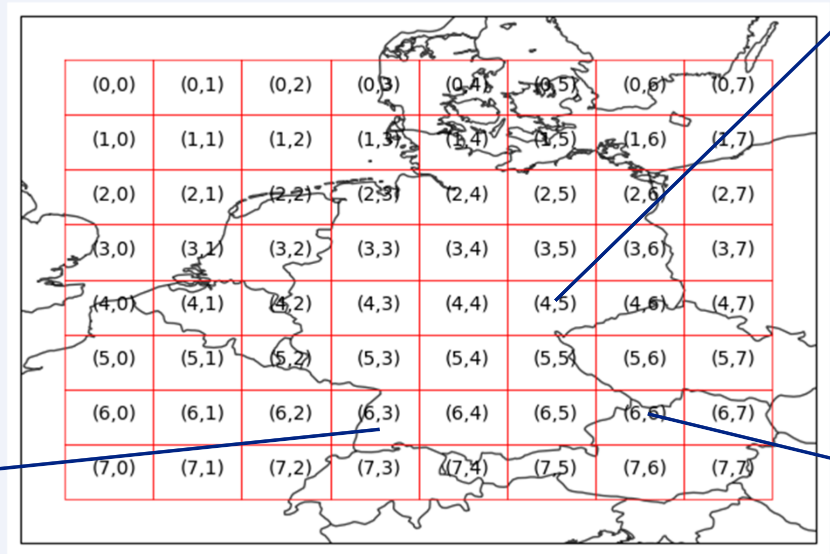

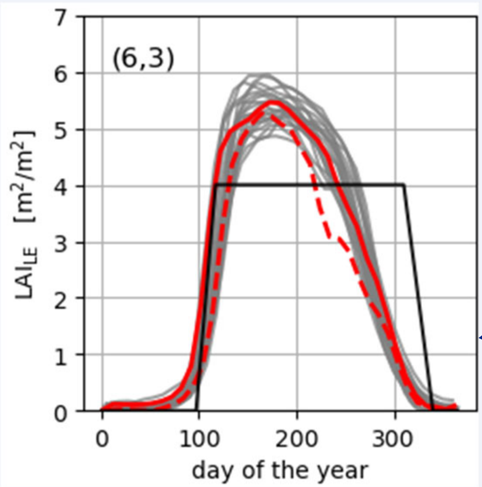

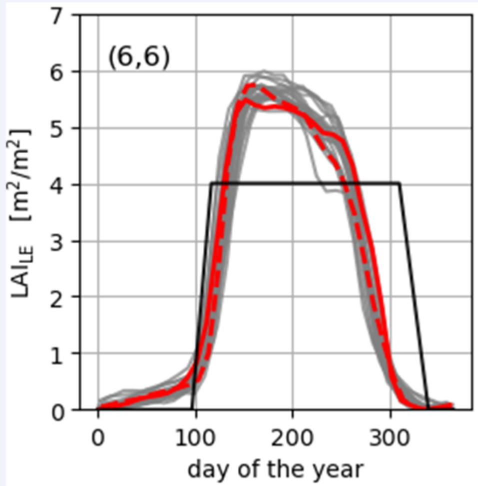

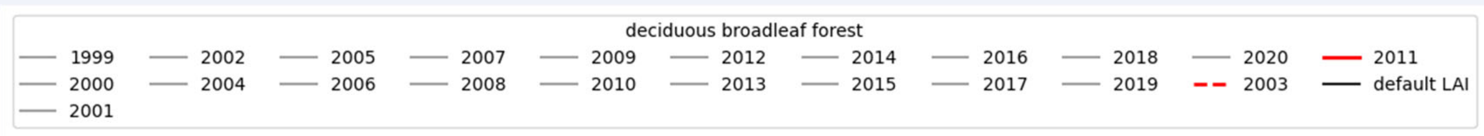

TNO innovation for life

Sensitivity Run in LOTOS-EUROS

LOTOS-EUROS v3.0.0

Resolution:

- 2019 including one month spin-up
- ~6 x 6 km^2 for the domain of Northwest Europe

Emissions:

- EU emission inventory CAMS v5.1 2018 [1], and for Germany the Greta emission inventory v1.2.0.1 from 2019 [2].
- Biogenic emissions using tree-specific emission factors, soil-NO_x emissions, sea salt emissions, desert dust, road resuspension and agricultural dust emissions and GFAS wildfire [3]
- Climatological boundaries from EMEP, Isaacson and Logan and 3-hourly results from the CAMS-nrt product.
- Time profiles from TEMPO v3.2 [4]

deciduous broadleaf lu-fraction

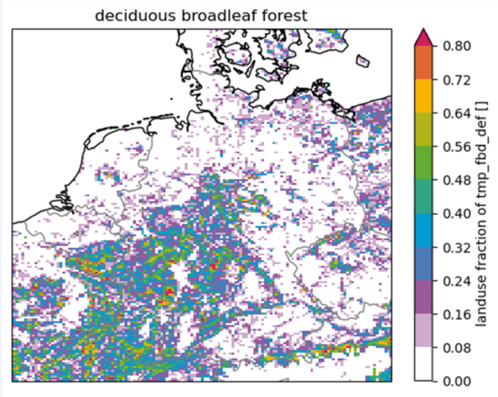

evergreen coniferous lu-fraction

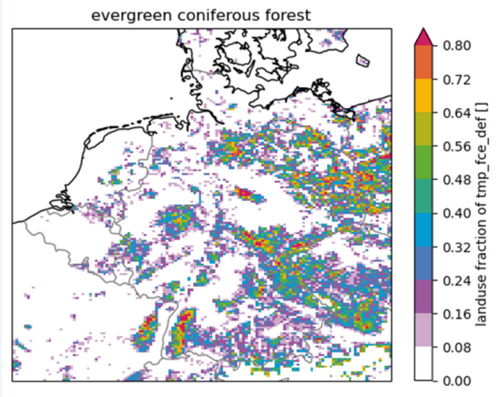

1. Soulie et al., 2024
2. Umweltbundesamt, 2022
3. Kaiser et al., 2012
4. Guevara et al., 2025

innovation for life

sensitivity run in LOTOS-EUROS

results: reduces NHx deposition

- overall reduction on NHx deposition ~0-5%
- ammonia peak in spring due to manure application
- deposition is most sensitive in spring
- south-west: broadleaf trees miss ammonia peak
- north-east: coniferous trees has overall lower LAI

daily avg. surface conc.

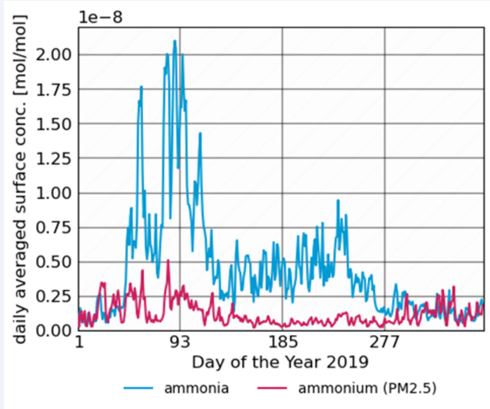

Satellite LAI   Satellite LAI/Ref

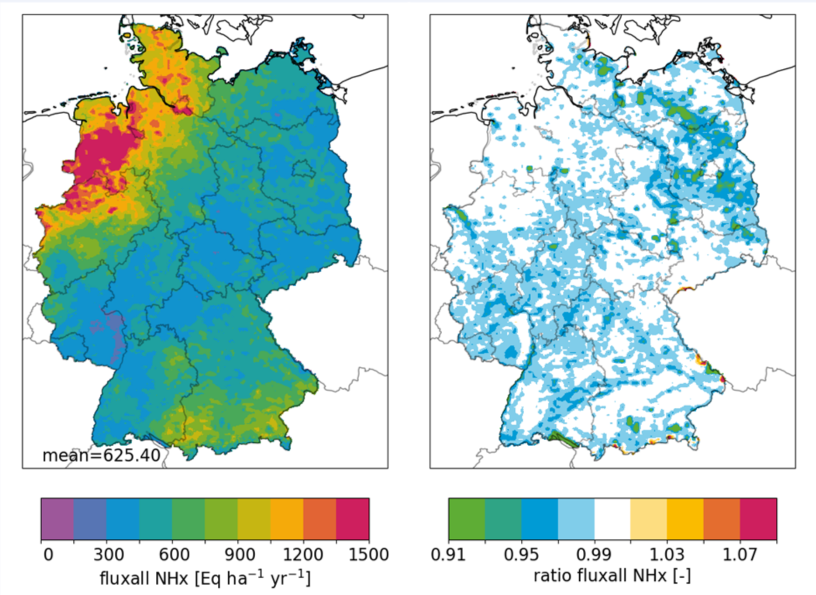

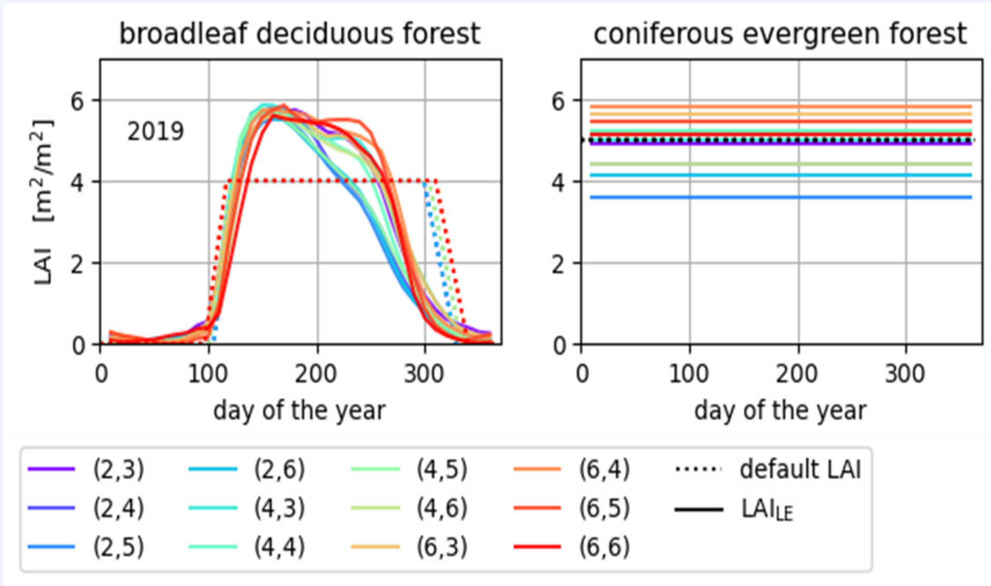

sensitivity run in LOTOS-EUROS

results: reduces NOy deposition

- overall reduction on NOy deposition ~0-5%
- NOy species relatively constant throughout the year
- south-west: broadleaf trees has lower LAI in winter, while heatwave in summer prevented to more dep.
- north-east: coniferous trees has overall lower LAI

daily avg. surface conc.

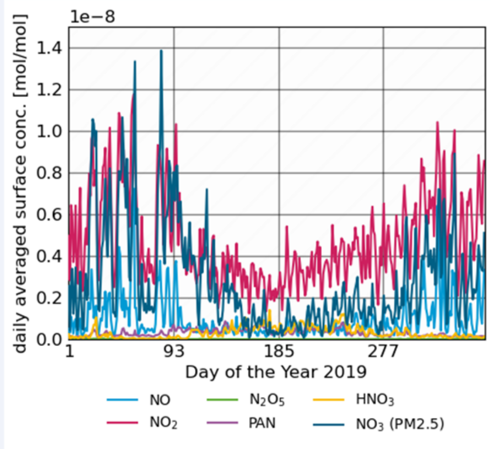

Satellite LAI

Satellite LAI / Ref

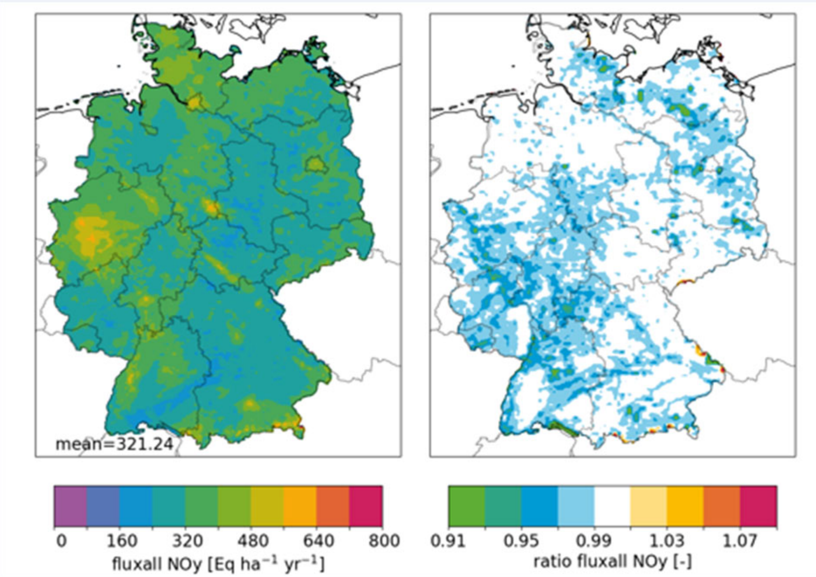

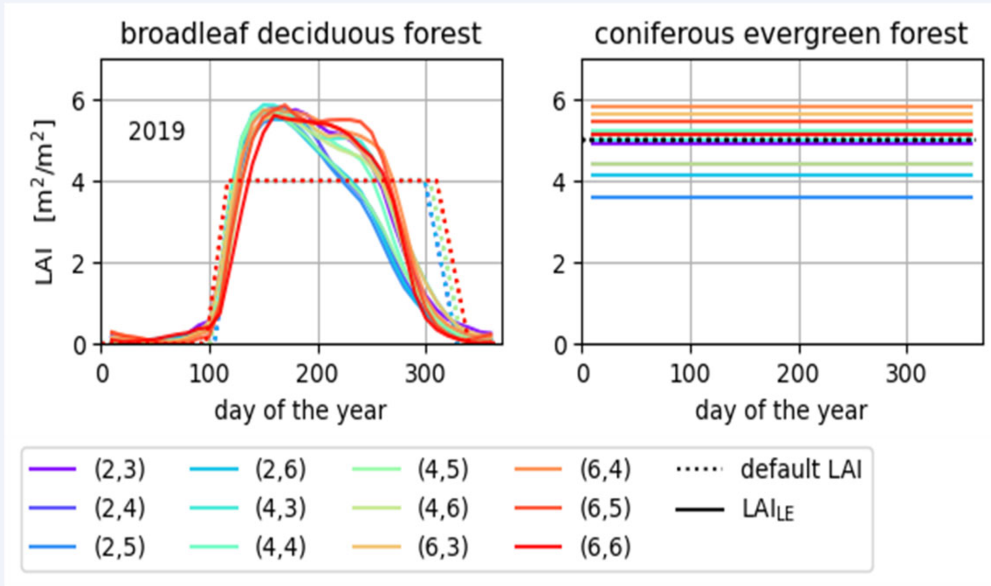

sensitivity run in LOTOS-EUROS

results: aerosol

- For ammonium nitrate aerosols form from NH_3 and NO_2
- Regions where both NHx and NOy deposition decreased, we observe increase of up to ~2% ammonium and nitrate PM2.5 aerosols.

SatelliteLAI

(SatelliteLAI - Ref) / Ref

ammonium

nitrate

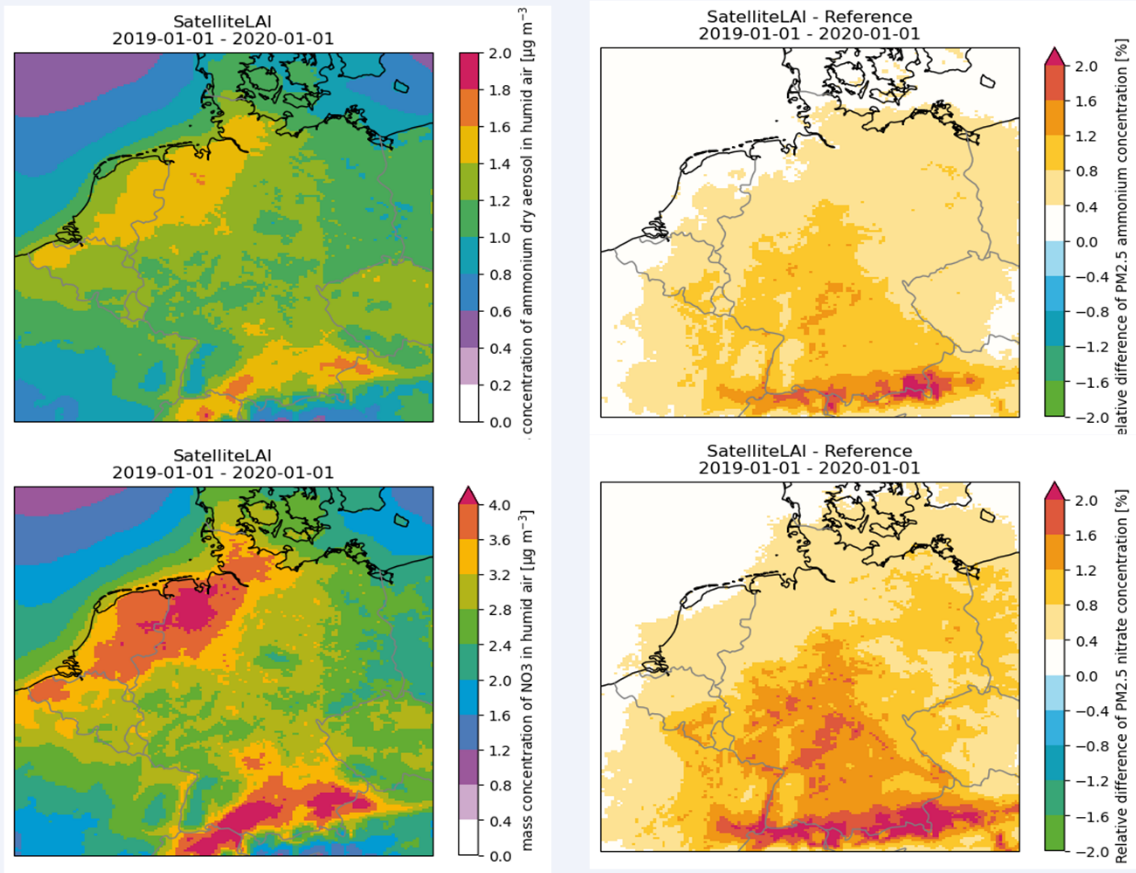

innovation for life

Conclusions

spatiotemporal variability in Satellite-derived forest LAI

coniferous forests show seasonality which is not realistic

broadleaf forests show non-zero LAI in winter

- spatial variability:
  - coniferous LAI: south > north
  - broadleaf LAI: growth and decay earlier in north

- temporal variability (broadleaf)
  - heatwave leads to faster decay of LAI
  - warm spring leads to earlier growth of LAI

Sensitivity Run

- spatial patterns and detailing appear in (ratio) concentration maps.
- NHx: sensitive to timing of LAI growth in spring for deciduous trees and lowered LAI for evergreen trees
- NOy: decreased area under LAI leads to lowered depositions.
- decreased NH3 and NO2 concentrations (0-5%) lead to decreased ammonium and nitrate PM2.5 up to ~2%.

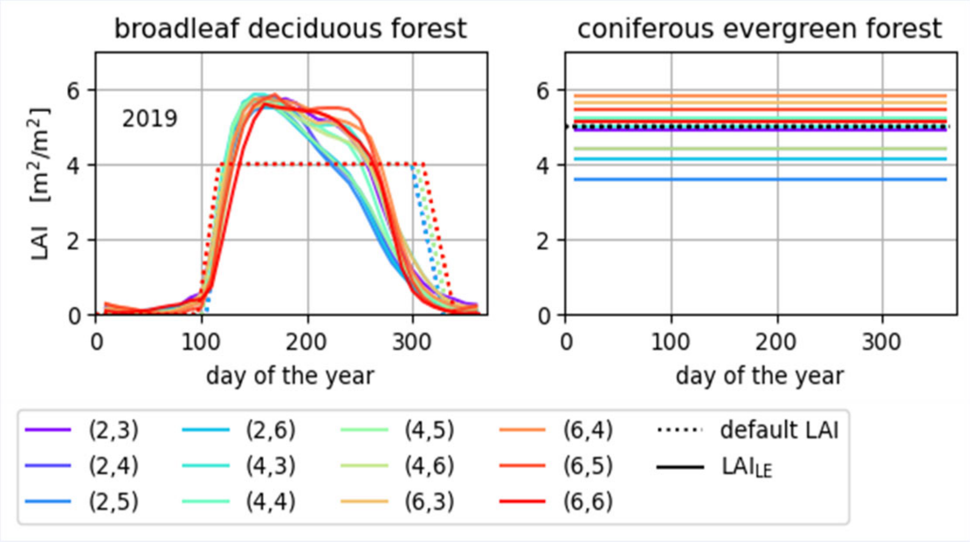

Current & future work

In this work, the coniferous evergreen and broadleaf deciduous trees are lumped together.

While part of the spatial dependency of LAI may be explained by the various tree species.

Therefore, LAI is sampled based on the tree species:

Fir, Alder, Birch, Beech, Larch, Pine, Oak, Spruce, Douglas Fir, Sessile and English Oak, and Scotch Pine.

dry flux N
coniferous evergreen forest
Satellite LAI / Ref

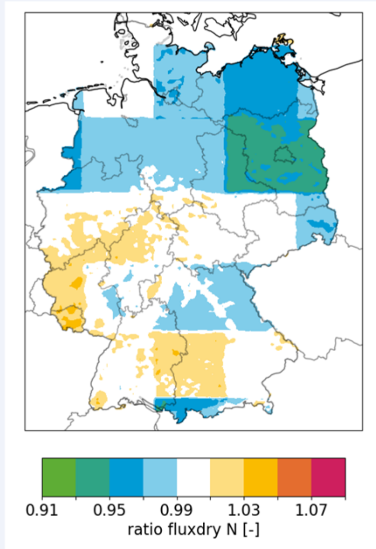

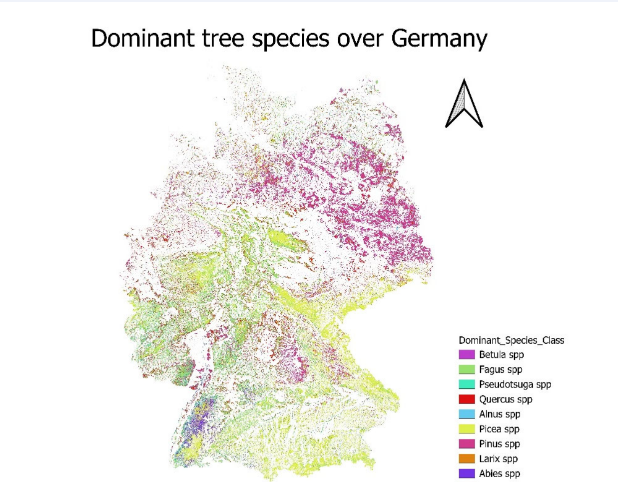

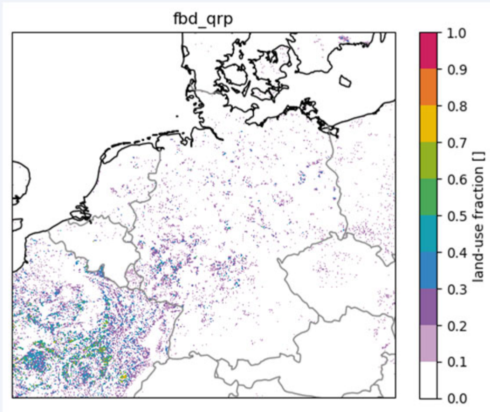

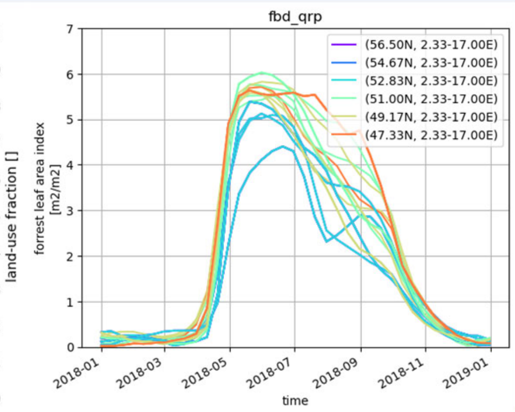

Blickensdörfer et al. (2024).

References

Blickensdörfer, L., Oehmichen, K., Pflugmacher, D., Kleinschmit, B., and Hostert, P.: National tree species mapping using Sentinel-1/2 time series and German National Forest Inventory data, Remote Sens. Environ., 304, 114069, https://doi.org/https://doi.org/10.1016/j.rse.2024.114069, 2024.

Forest Type 2018 (raster 10 m, 100 m), Europe, 3-yearly – Copernicus Land Monitoring Service: https://land.copernicus.eu/en/products/high-resolution-layer-forests-and-tree-cover/forest-type-2018-raster-10-m-100-m-europe-3-yearly, last access: 21 May 2025.

Kaiser, J. W., Heil, A., Andreae, M. O., Benedetti, A., Chubarova, N., Jones, L., Morcrette, J.-J., Razinger, M., Schultz, M. G., Suttie, M., and van der Werf, G. R.: Biomass burning emissions estimated with a global fire assimilation system based on observed fire radiative power, Biogeosciences, 9, 527–554, https://doi.org/10.5194/bg-9-527-2012, 2012.

Soulie, A., Granier, C., Darras, S., Zilbermann, N., Doumbia, T., Guevara, M., Jalkanen, J.-P., Keita, S., Liousse, C., Crippa, M., Guizzardi, D., Hoesly, R., and Smith, S. J.: Global anthropogenic emissions (CAMS-GLOB-ANT) for the Copernicus Atmosphere Monitoring Service simulations of air quality forecasts and reanalyses, Earth Syst. Sci. Data, 16, 2261–2279, https://doi.org/10.5194/essd-16-2261-2024, 2024.

Verger, A., Sánchez-Zapero, J., Weiss, M., Descals, A., Camacho, F., Lacaze, R., and Baret, F.: GEOV2: Improved smoothed and gap filled time series of LAI, FAPAR and FCover 1 km Copernicus Global Land products, Int. J. Appl. Earth Obs. Geoinf., 123, 103479, https://doi.org/https://doi.org/10.1016/j.jag.2023.103479, 2023.

Umweltbundesamt: German Informative Inventory Report 2022 (IIR 2022)., 2022.

Zhang, L., Gong, S., Padro, J., and Barrie, L.: A size-segregated particle dry deposition scheme for an atmospheric aerosol module, Atmos. Environ., 35, 549–560, https://doi.org/https://doi.org/10.1016/S1352-2310(00)00326-5, 2001.

van Zanten, M. C. van, Sauter, F. J., Kruit, R. J. W., JA. van Jaarsveld, P., and Pul, W. A. J. van: Description of the DEPAC module, 1–76, 2010.

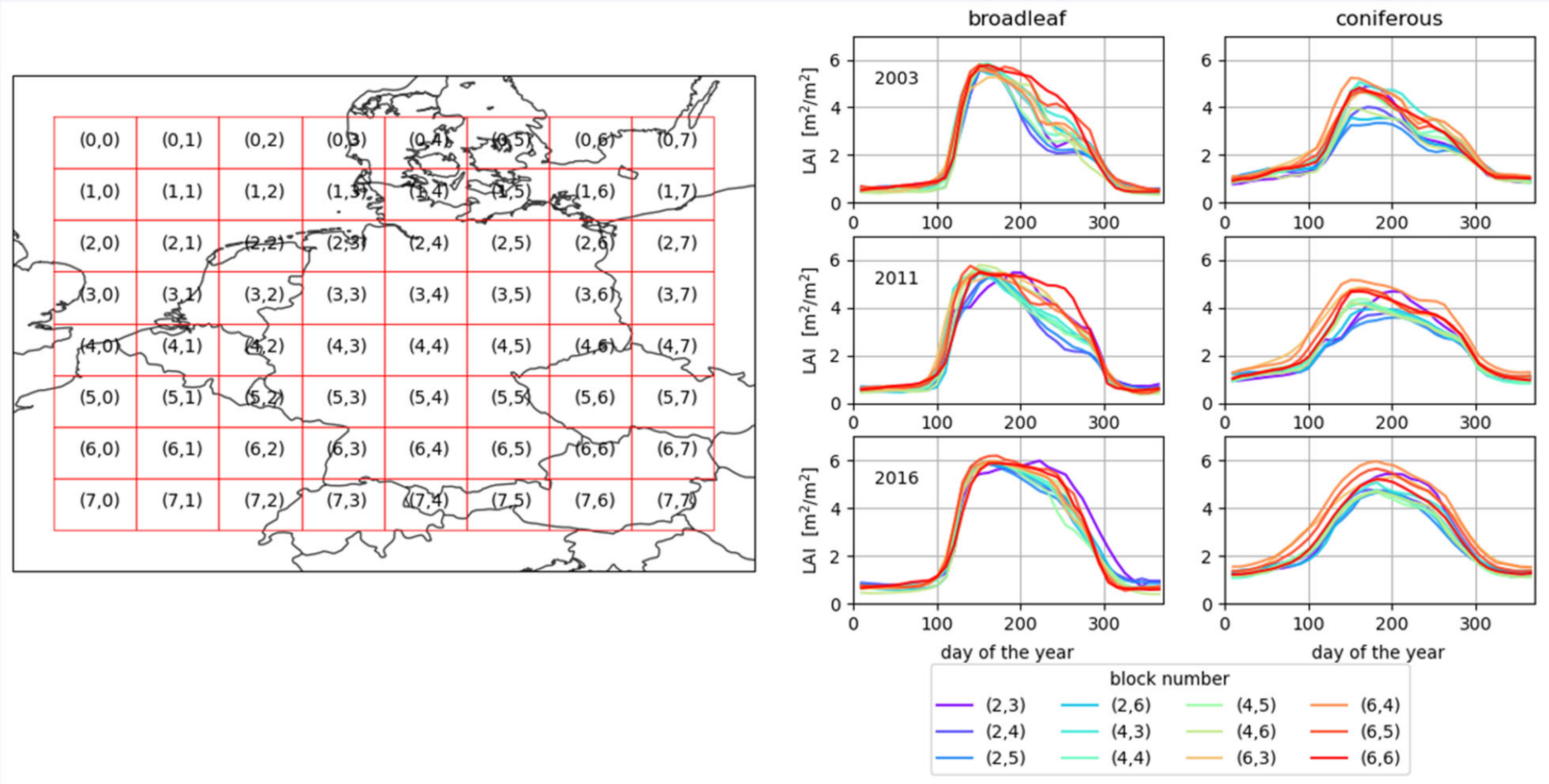
(0,0) (0,1) (0,2) (0,3) (0,4) (0,5) (0,6) (0,7)
(1,0) (1,1) (1,2) (1,3) (1,4) (1,5) (1,6) (1,7)
(2,0) (2,1) (2,2) (2,3) (2,4) (2,5) (2,6) (2,7)
(3,0) (3,1) (3,2) (3,3) (3,4) (3,5) (3,6) (3,7)
(4,0) (4,1) (4,2) (4,3) (4,4) (4,5) (4,6) (4,7)
(5,0) (5,1) (5,2) (5,3) (5,4) (5,5) (5,6) (5,7)
(6,0) (6,1) (6,2) (6,3) (6,4) (6,5) (6,6) (6,7)
(7,0) (7,1) (7,2) (7,3) (7,4) (7,5) (7,6) (7,7)
broadleaf
coniferous
2003
2011
2016
LAI [m^2/m^2]
day of the year
block number
(2,3) (2,4) (2,5) (2,6) (4,3) (4,4) (4,5) (4,6) (6,3) (6,4) (6,5) (6,6)